

Muon rates in UA1, D0, CDF and CMS predicted by PYTHIA 5.7

M. Ćwiok

Institute of Experimental Physics, Warsaw University, Poland

G. Wrochna

CERN, Geneva, Switzerland

Abstract

We present a comparison of muon and b-quark spectra calculated by PYTHIA 5.7 event generator with CDF, D0 and UA1 experimental results. New predictions on hadron and muon rates for the LHC energy are given. Possible impact on the CMS muon trigger design is briefly discussed.

1 Introduction

The previous estimates [2, 3] of hadron and prompt muon rates have been done with PYTHIA 5.6 event generator. In the version 5.7 new structure functions have been implemented following HERA results at low x , and some parameters have been tuned in order to reproduce the recent experimental data. In this note we compare PYTHIA predictions with recent CDF and D0 results, as well as with previous UA1 measurements of b-quark and muon inclusive cross sections. We predict the muon rates in LHC p-p collisions at $\sqrt{s} = 14$ TeV. For the purpose of the design of the CMS muon trigger new parametrisations of hadron and muon rates are proposed.

2 Details of simulation

Rates of particles produced at the vertex have been estimated with PYTHIA generator for

- p- \bar{p} events at $\sqrt{s} = 630$ GeV, $\sqrt{s} = 1.8$ TeV
- p-p events at $\sqrt{s} = 14$ TeV.

In the previous studies [2, 3] PYTHIA parameters have been tuned to reproduce UA1 minimum bias data [4]

```
MSEL          = 1                ! "min-bias"
MSTP (82) = 4
MSTP ( 2) = 2
MSTP (33) = 3
PARP (85) = 0.81
PARP (86) = 0.9
PARP (82) = 1.6
```

In the present study PYTHIA default parameters have been used throughout [5]. We have simulated the following processes with parameters listed below

- Minimum bias events including
 - $q_i q_j \rightarrow q_i q_j$ (where $q_i = d, u, s, c, b$)
 - $q_i \bar{q}_i \rightarrow q_i \bar{q}_i$
 - $q_i \bar{q}_i \rightarrow g g$
 - $q_i g \rightarrow q_i g$
 - $g g \rightarrow q_i \bar{q}_i$
 - $g g \rightarrow g g$
 - low p_t scattering

with parameter

```
MSEL = 1                                ! "min-bias"
```

- Drell-Yan events with

```
MSEL      = 0
MSUB( 1) = 1                                ! "Drell-Yan"
MSTP(43) = 1                                ! "only gamma* included"
```

- Single W,Z production events with

```
MSEL      = 0
MSUB( 1) = 1
MSUB( 2) = 1
MSUB( 15) = 1
MSUB( 16) = 1
MSUB( 19) = 1
MSUB( 20) = 1
MSUB( 30) = 1
MSUB( 31) = 1
MSUB( 35) = 1
MSUB( 36) = 1
MSUB(131) = 1
MSTP( 43) = 2                                ! "only Z0 included"
```

- Top quark production events with

```
MSEL      = 6                                ! "top production"
PMAS(6,1) = 180.                            ! "top mass = 180 GeV"
PMAS(LUCOMP(661),1) = 360.
PMAS(LUCOMP(663),1) = 360.
PMAS(LUCOMP(665),1) = 360.
PMAS(LUCOMP(10661),1) = 360.
PMAS(LUCOMP(10663),1) = 360.
PMAS(LUCOMP(20663),1) = 360.
```

Table 1 summarizes number of generated events and cross sections calculated by PYTHIA for each type of processes.

In the following analysis we treat π^\pm, K_L^0, K^\pm as stable particles. The percentage of final state (undecayed) hadrons from minimum bias events at the LHC energy is listed in Table 2.

Table 1: Number of generated events and PYTHIA cross sections obtained for: p- \bar{p} collisions at 630 GeV, 1.8 TeV and p-p collisions at 14 TeV.

Process	Events generated	Cross section [mb]
p-\bar{p} $\sqrt{s} = 630$ GeV		
Minimum bias	$15 \cdot 10^6$	33.02
Minimum bias ($p_T^{jet} > 10$ GeV)	$4 \cdot 10^6$	$7.93 \cdot 10^{-2}$
Minimum bias ($p_T^{jet} > 30$ GeV)	10^6	$4.17 \cdot 10^{-4}$
Drell-Yan	$2 \cdot 10^6$	$1.22 \cdot 10^{-4}$
W,Z production	10^6	$1.41 \cdot 10^{-5}$
p-\bar{p} $\sqrt{s} = 1.8$ TeV		
Minimum bias	$10 \cdot 10^6$	39.00
Minimum bias ($p_T^{jet} > 10$ GeV)	$2 \cdot 10^6$	$4.34 \cdot 10^{-1}$
Minimum bias ($p_T^{jet} > 30$ GeV)	10^6	$4.95 \cdot 10^{-3}$
Drell-Yan	$2 \cdot 10^6$	$2.49 \cdot 10^{-4}$
W,Z production	10^6	$5.70 \cdot 10^{-5}$
p-p $\sqrt{s} = 14$ TeV		
Minimum bias	$2 \cdot 10^6$	55.19
Minimum bias ($p_T^{jet} > 10$ GeV)	10^6	6.04
Minimum bias ($p_T^{jet} > 30$ GeV)	10^6	$1.48 \cdot 10^{-1}$
Drell-Yan	$2 \cdot 10^6$	$9.77 \cdot 10^{-4}$
W,Z production	10^6	$5.81 \cdot 10^{-4}$
Top quark production ($m_{top} = 180$ GeV)	$2 \cdot 10^5$	$5.24 \cdot 10^{-7}$

Table 2: Percentage of final state hadrons generated by PYTHIA for minimum bias p-p events at 14 TeV.

Particle type	Fraction generated
π^\pm	63.23%
K_L^0, K_S^0	10.54%
K^\pm	10.74%
p, \bar{p}	7.84%
n, \bar{n}	7.65%

3 Inclusive b-quark spectra from CDF, D0 and UA1

It has been shown [6] that the prompt muon spectrum (except very low p_t) is dominated by charm and beauty decays. Thus it is important to check whether PYTHIA results agree with the existing experimental data on muon and b-quark production in p- \bar{p} colliders [7, 8, 9, 10, 11]. Figures 1 and 2 show p_t^b distribution of b quarks ($Q=-\frac{1}{3}$) coming from minimum bias events (filled circles). It is seen that above 10 GeV, the statistical fluctuations are high. It was necessary to generate additional data sets with requirements of $p_t^{jet} > 10$ GeV and $p_t^{jet} > 30$ GeV (opened triangles and squares respectively). The resulting sample of b-quarks is composed of 3 components:

- $p_t^b < 12$ GeV from minimum bias sample without p_t^{jet} cut,
- $12 \text{ GeV} < p_t^b < 50$ GeV from $p_t^{jet} > 10$ GeV sample,
- $p_t^b > 50$ GeV from $p_t^{jet} > 30$ GeV sample.

For the relative normalisation of these subsamples we have used the PYTHIA calculated total cross sections (see Table 1). The same rapidity cuts as in the experiments have been applied, namely $|\eta^b| < 1.0$ for CDF and D0, $|\eta^b| < 1.5$ for UA1. The results are plotted in Figures 3 and 4 (full circles). A contribution of b quarks coming from Drell-Yan and W,Z events is also shown.

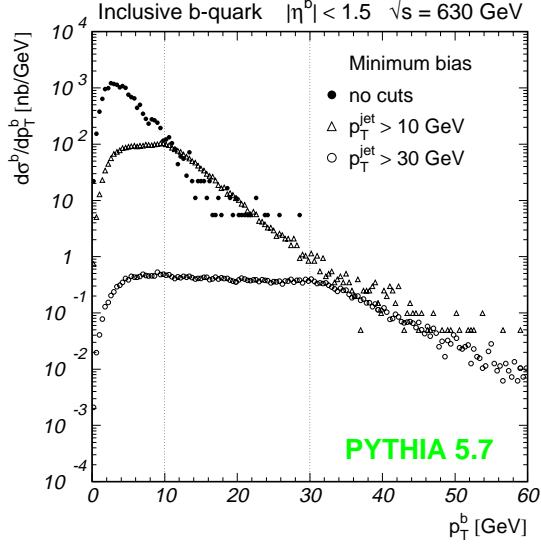


Figure 1: Inclusive b-quark p_t spectra from minimum bias events simulated with PYTHIA at 630 GeV.

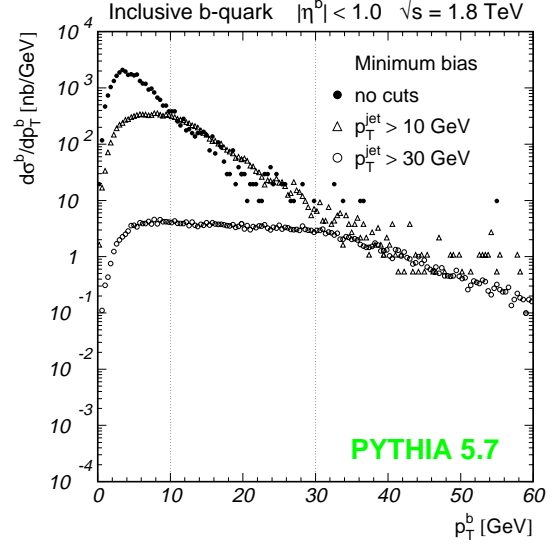


Figure 2: Inclusive b-quark p_t spectra from minimum bias events simulated with PYTHIA at 1.8 TeV.

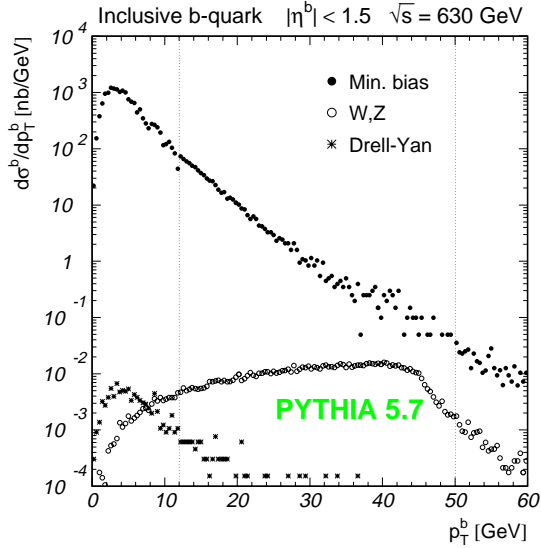


Figure 3: Contributions to the inclusive b-quark p_t spectrum from minimum bias, Drell-Yan and W,Z production simulated with PYTHIA at 630 GeV.

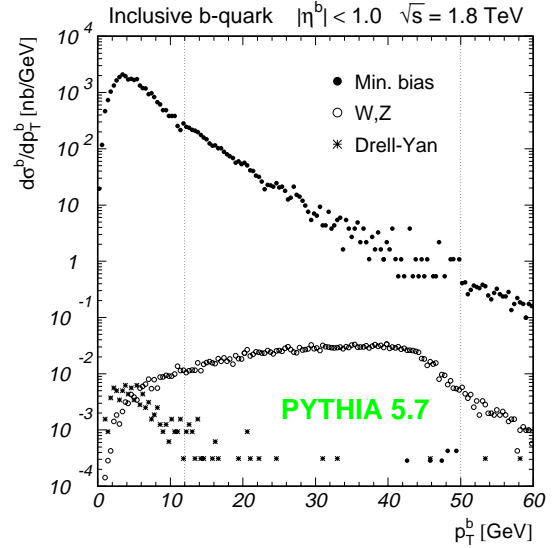


Figure 4: Contributions to the inclusive b-quark p_t spectrum from minimum bias, Drell-Yan and W,Z production simulated with PYTHIA at 1.8 TeV.

Figures 5 and 6 compare an integrated cross section $\sigma^{p\bar{p} \rightarrow b+X}(p_t^b > p_t^{min})$ calculated by PYTHIA with experimental data from CDF, D0 and UA1 collaborations. It can be seen that UA1 data agree rather well with simulations. Spectrum measured by D0 is also well reproduced, whereas the CDF data diverge slightly at low p_t^{min} .

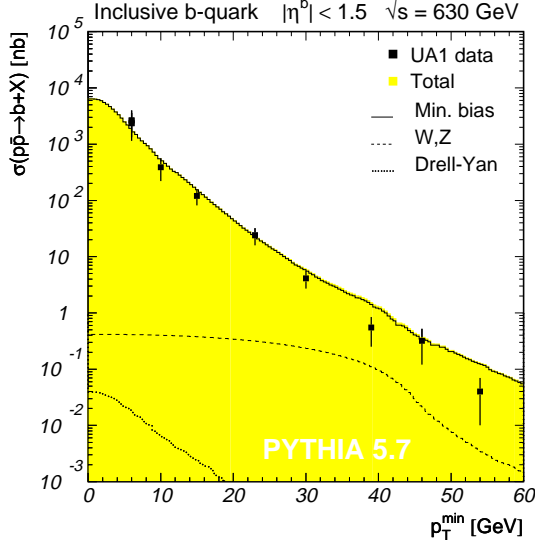


Figure 5: Integrated inclusive b-quark ($Q=-\frac{1}{3}$) cross section simulated with PYTHIA at 630 GeV compared with UA1 data.

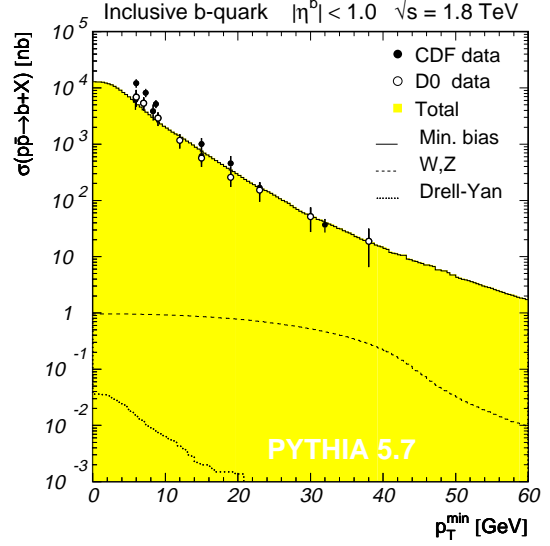


Figure 6: Integrated inclusive b-quark ($Q=-\frac{1}{3}$) cross section simulated with PYTHIA at 1.8 TeV compared with CDF and D0 data.

4 Inclusive muon spectra from b-decays from D0 and UA1

The similar method have been applied to obtain the p_t spectra of muons originating from the beauty decays (muons and b-quarks of both signs). The rapidity cuts used were identical with experimental ones, namely $|\eta^\mu| < 0.8$ for D0, $|\eta^\mu| < 1.5$ for UA1. Cross sections have been normalized to one unit of rapidity. The p_t spectra of muons obtained from the minimum bias (open squares), $p_T^{jet} > 10$ GeV (open triangles) and $p_T^{jet} > 30$ GeV (open circles) events are plotted in Figures 7 and 8. Thereafter, we have used three subsamples of muons

- $p_t^b < 6$ GeV from minimum bias sample without p_T^{jet} cut,
- $6 \text{ GeV} < p_t^b < 16$ GeV from $p_T^{jet} > 10$ GeV sample,
- $p_t^b > 16$ GeV from $p_T^{jet} > 30$ GeV sample.

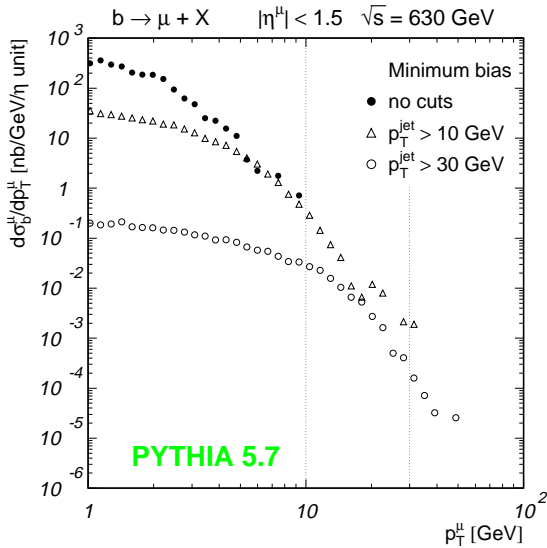


Figure 7: Inclusive muon from beauty decays p_t spectra from minimum bias events simulated with PYTHIA at 630 GeV.

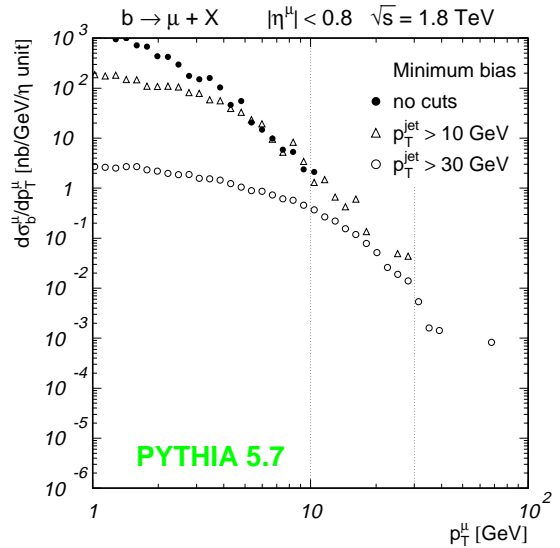


Figure 8: Inclusive muon from beauty decays p_t spectra from minimum bias events simulated with PYTHIA at 1.8 TeV.

The total calculated cross sections $d\sigma^{p\bar{p} \rightarrow b \rightarrow \mu+X}/dp_t^\mu$ for SPS and Tevatron are shown in Fig. 9 and 10 respectively. Contributions of Drell-Yan and W,Z production events are indicated as well. The results are compared with UA1 (full squares) and D0 (full circles) data. We lack statistics in the high p_t^μ region, but within the errors the agreement is satisfactory.

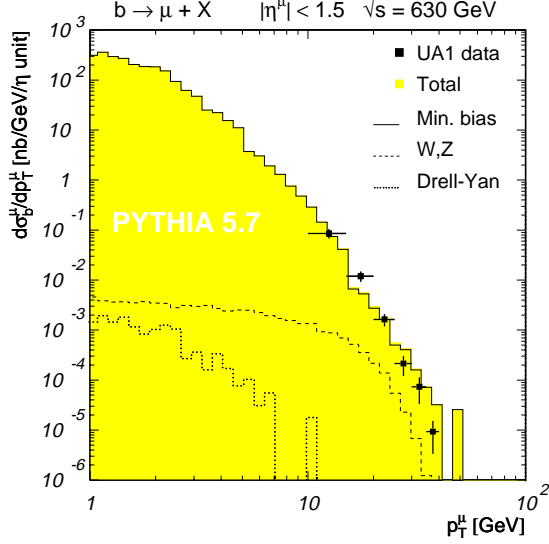


Figure 9: Inclusive muon $d\sigma^{p\bar{p} \rightarrow b \rightarrow \mu+X}/dp_t^\mu$ simulated with PYTHIA at 630 GeV in comparison with UA1 data.

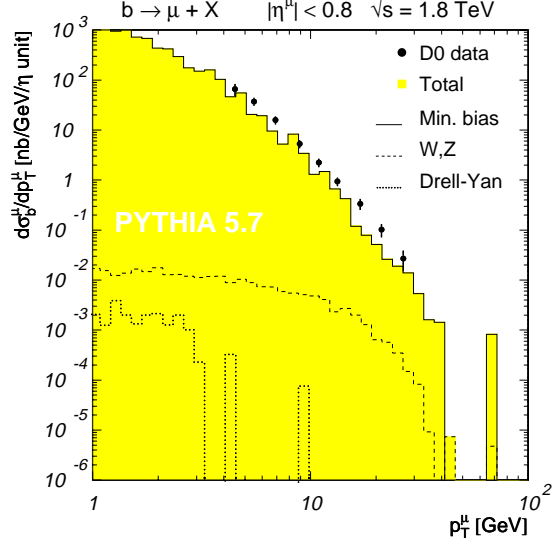


Figure 10: Inclusive muon $d\sigma^{p\bar{p} \rightarrow b \rightarrow \mu+X}/dp_t^\mu$ simulated with PYTHIA at 1.8 TeV in comparison with D0 data.

Integrated muon spectra from b-decays for SPS and Tevatron are plotted in Figures 11 and 12 respectively. Cross sections measured in several p_t^μ bins described in Ref. [7, 9] have been used to calculate integrated spectra for UA1 and D0. It can be seen from figures that for D0 agreement is satisfactory, whereas σ predicted for UA1 at $p_t^{\min} > 20$ GeV is higher than the data. Fig. 9 indicates however that this may be caused by statistical fluctuations.

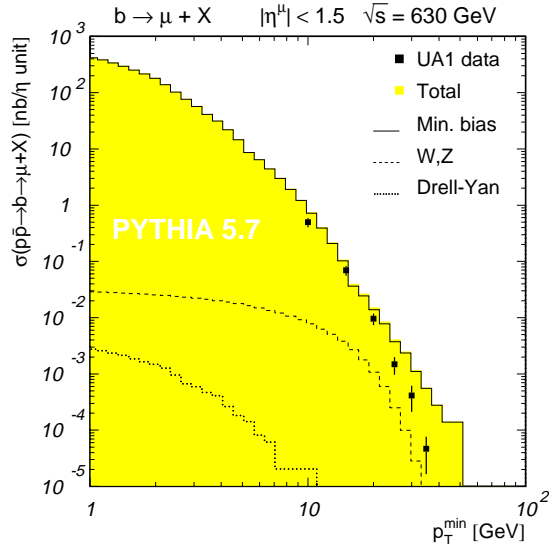


Figure 11: Integrated inclusive muon cross section simulated with PYTHIA at 630 GeV in comparison with UA1 data.

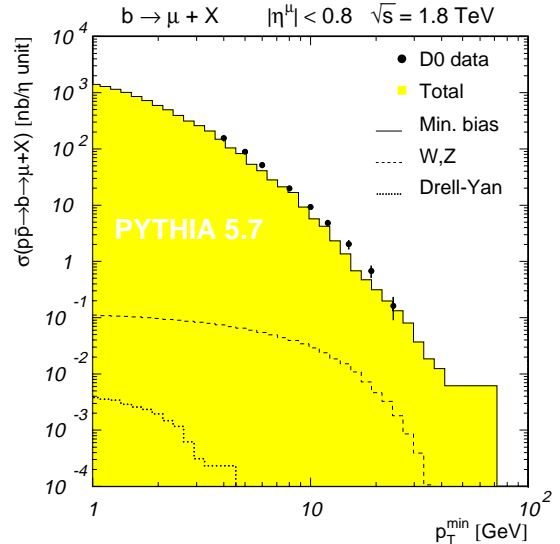


Figure 12: Integrated inclusive muon cross section simulated with PYTHIA at 1.8 TeV in comparison with D0 data.

5 Inclusive total muon spectra from D0 and UA1

We define prompt muons as muons originating from: beauty and charm decays, Drell-Yan, τ -lepton decays and light quarks resonances (ρ , ϕ , η). Muons from the W,Z decays have been treated separately because of the different shape of their p_t spectrum. A background coming from π^\pm , K_L^0 , K^\pm decays within Central Tracking Detector volume have been also estimated (length of $L = 1.7$ m and radius of $R = 0.8$ m have been assumed for D0).

For the minimum bias muon sample we followed the procedure described in Sec. 4. In addition Drell-Yan and W,Z events have been calculated. Figure 13 shows $d\sigma^{p\bar{p} \rightarrow \mu+X}/dp_t^\mu$ (without π/K decay contribution) compared with UA1 data. Prompt (solid line) and W,Z (dotted line) muons are indicated. Figure 14 illustrates: prompt muons (solid line), muons from W,Z (dotted line) and the contribution from π/K decays (dashed line) compared with D0 measurements.

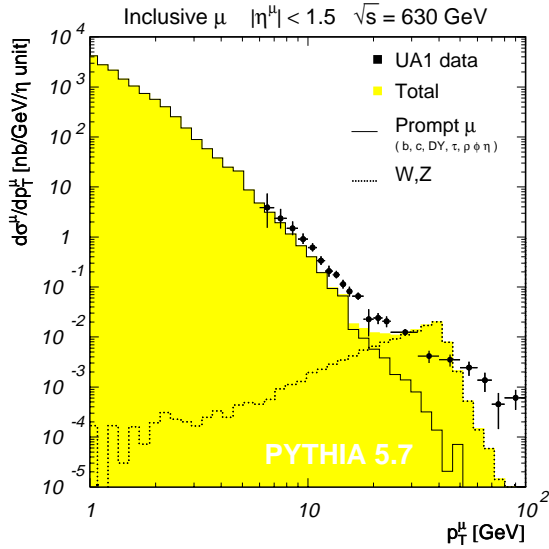


Figure 13: Total inclusive muon $d\sigma^{p\bar{p} \rightarrow \mu+X}/dp_t^\mu$ simulated with PYTHIA at 630 GeV in comparison with UA1 data (without π/K decay contribution). Experimental points are not corrected for detector resolution.

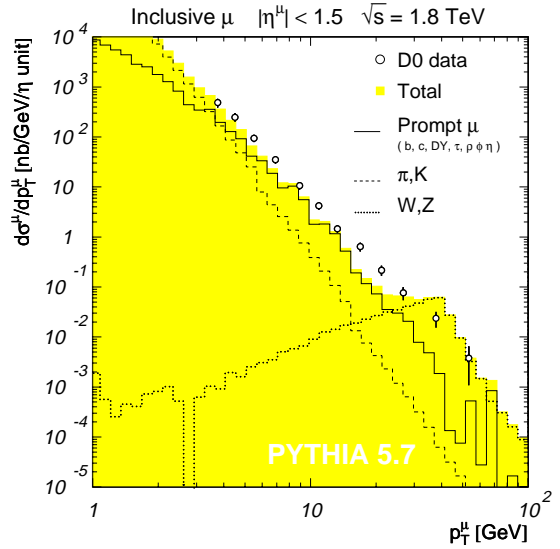


Figure 14: Total inclusive muon $d\sigma^{p\bar{p} \rightarrow \mu+X}/dp_t^\mu$ simulated with PYTHIA at 1.8 TeV in comparison with D0 data (with π/K decay contribution). Experimental points are not corrected for detector resolution.

It is evident that muons coming from W,Z bosons dominate in high p_t^μ region. However simulated spectrum has a narrow peak at about 40 GeV not seen in the experimental data. This discrepancy seems to be understood since the UA1 and D0 points are smeared due to detector resolution. To correct for this effect we assumed a gaussian distribution of a variable $q = p_t^{-1}$ with a variance σ_q^2 and we smeared the p_t^μ spectra.

For UA1 we assumed linear behaviour of $\sigma_q(p_t)$, namely

$$\frac{\sigma_q}{q} = 0.01 \cdot p_t [\text{GeV}].$$

For D0 we used parametrisations published in Ref. [11]

$$\frac{\sigma_q}{q} = \sqrt{\left(0.18 \frac{p_t - 2}{p_t}\right)^2 + (0.008 p_t)^2}$$

where p_t is expressed in GeV. Then corrected distributions are presented in plots 15 and 16.

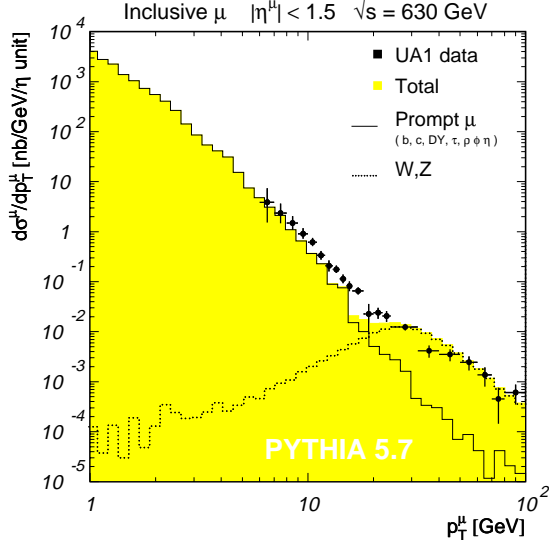


Figure 15: Total inclusive muon $d\sigma^{p\bar{p} \rightarrow \mu+X}/dp_t^\mu$ simulated with PYTHIA at 630 GeV with smeared p_t^μ spectrum in comparison with UA1 data (without π/K decay contribution). Experimental points are not corrected for detector resolution.

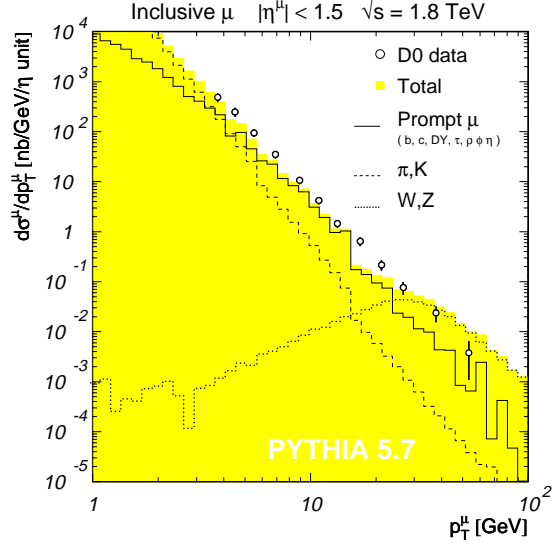


Figure 16: Total inclusive muon $d\sigma^{p\bar{p} \rightarrow \mu+X}/dp_t^\mu$ simulated with PYTHIA at 1.8 TeV with smeared p_t^μ spectrum in comparison with D0 data (with π/K decay contribution). Experimental points are not corrected for detector resolution.

6 Muon and hadron rates at the LHC

In order to see how hadron and muons rates predicted by PYTHIA vary with \sqrt{s} we compared integrated cross sections of b-quark and muons from b-decays for several p_t^{min} values at SPS, Tevatron and LHC energies. Fig. 17 shows integrated b-quark ($Q=-\frac{1}{3}$) spectrum normalized to one unit of rapidity for $p_t^{min} = 6, 10, 15, 20, 25, 30, 35$ GeV. For each p_t^{min} value simulated cross sections at $\sqrt{s} = 630$ GeV, 1.8 TeV and 14 TeV are connected with solid line (corresponding error bounds are indicated with dotted lines). Similar procedure as described in Sec. 3 have been applied to obtain b-quark spectrum at the LHC energy. To plot experimental points for Tevatron we used an average of CDF and D0 measurements (shown in Fig. 6) and maximal error bounds. Thereafter we interpolate existing UA1 data and averaged CDF and D0 data to calculate cross sections at $p_t^{min} = 6, 10, 15, 20, 25, 30, 35$ GeV.

Fig. 18 illustrates integrated muon spectra from b-decays (muons and b-quarks of both signs) normalized to one unit of rapidity for $p_t^{min} = 5, 10, 15, 20, 25, 30$ GeV. Analogous method as described in Sec. 4 have been used to obtain muon spectrum at the LHC energy. For each p_t^{min} value simulated cross sections at $\sqrt{s} = 630$ GeV, 1.8 TeV and 14 TeV are connected with solid line (corresponding error bounds are indicated with dotted lines). To plot data points the measurements from UA1 and D0 (shown in Figures 11 and 12) have been interpolated to obtain cross sections for $p_t^{min} = 5, 10, 15, 20, 25, 30$ GeV.

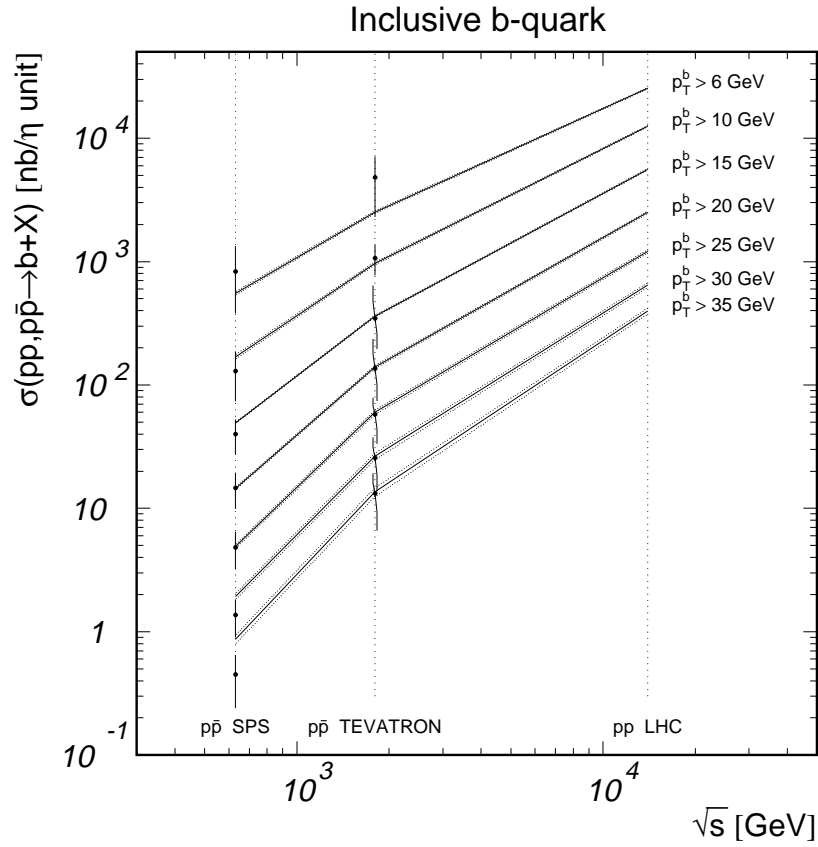


Figure 17: Comparison of integrated b-quark ($Q = -\frac{1}{3}$) cross sections calculated with PYTHIA with interpolated experimental data from SPS and Tevatron for several p_t^{min} values.

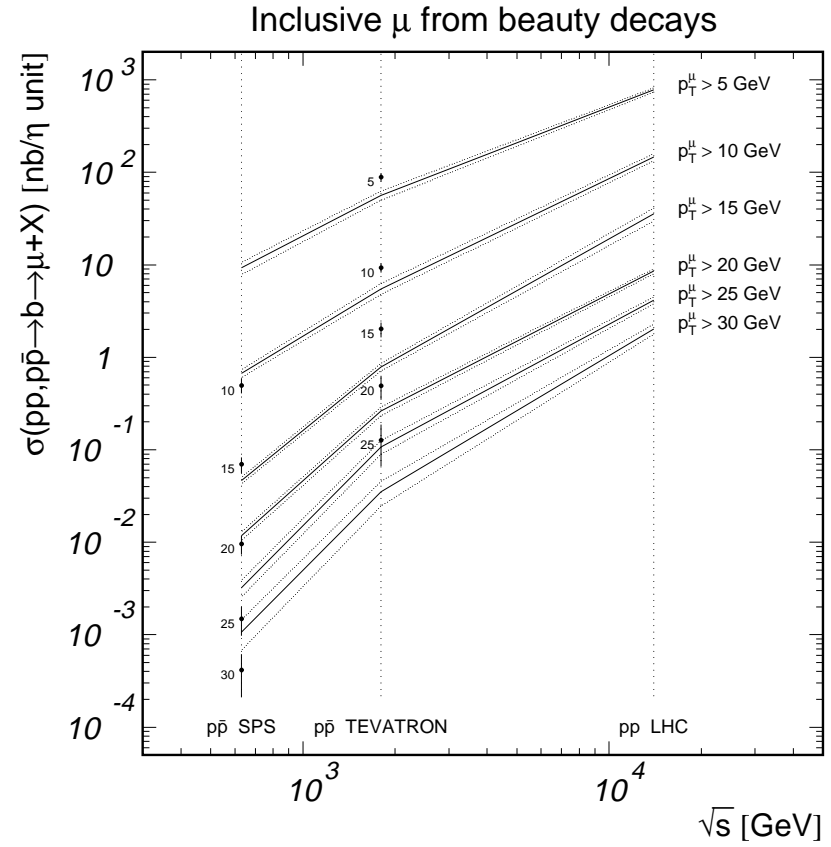


Figure 18: Comparison of integrated cross sections of muons from beauty decays calculated with PYTHIA with interpolated experimental data from SPS and Tevatron for several p_t^{min} values.

The p_t and η distributions of produced hadrons and prompt muons at the LHC energy are shown in Fig. 19. It is seen that the rapidity spectrum in the interesting region of $|\eta| < 3.0$ is flat, thus the p_t spectrum can be regarded as rapidity independent. Luminosity of $10^{34} \text{ cm}^{-2}\text{s}^{-1}$ have been assumed to estimate the particle rates.

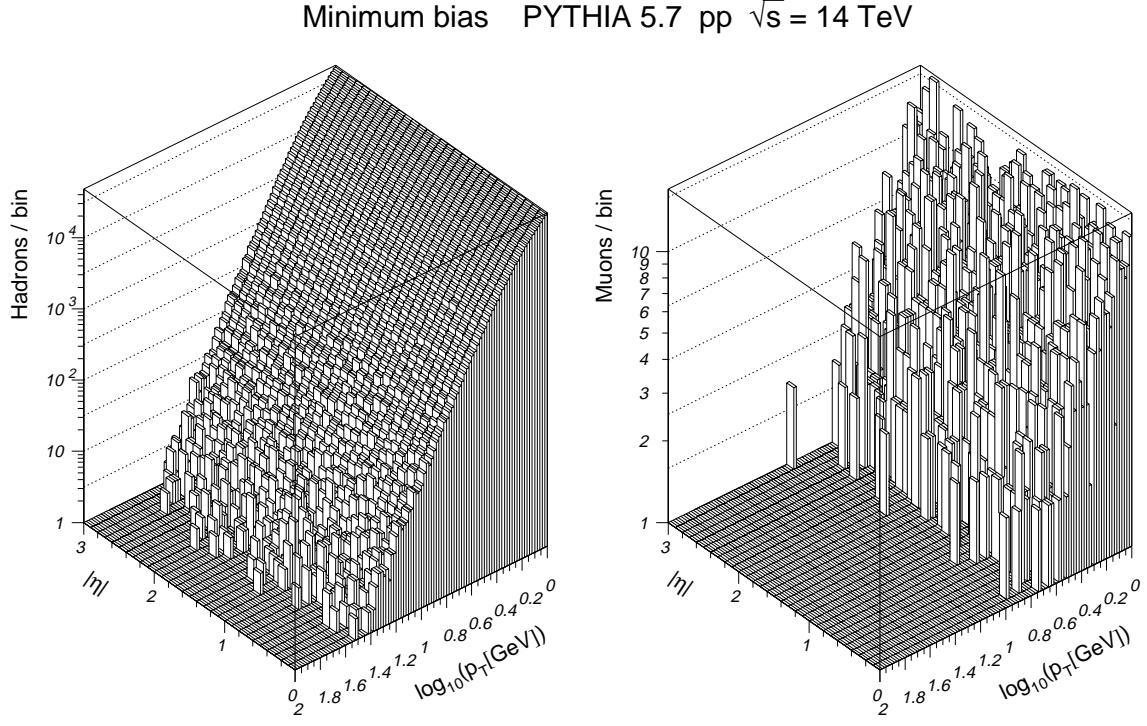


Figure 19: Rapidity distribution of hadrons and muons from minimum bias events simulated with PYTHIA 5.7 at 14 TeV.

The p_t distribution of hadrons normalized to one unit of rapidity is shown in Fig. 20 (full circles). In addition, the hard p_t events of $p_t^{jet} > 30 \text{ GeV}$ (open circles) have been simulated in order to reduce fluctuations at the tail (see Table 1). Thereafter, a distribution to be parametrized consists of minimum bias events below $p_t < 30 \text{ GeV}$ and of hard events above that. It is shown in Fig. 21.

The spectrum of hadrons has been fitted with the following formula:

$$\frac{dN}{d\eta dp_t} = a (p_t^\alpha + b)^\beta$$

where

$$a = 1.1429 \cdot 10^{10}, \quad b = 0.8251, \quad \alpha = 1.306, \quad \beta = -3.781.$$

The distribution is given in $[\text{GeV}^{-1}\cdot\text{s}^{-1}]$. Result of the fit is plotted in Fig. 22. The above formula has no physical meaning, except that at high p_t it exhibits well known behaviour of $p_t^{-\alpha}$, where $\alpha \approx 5$.

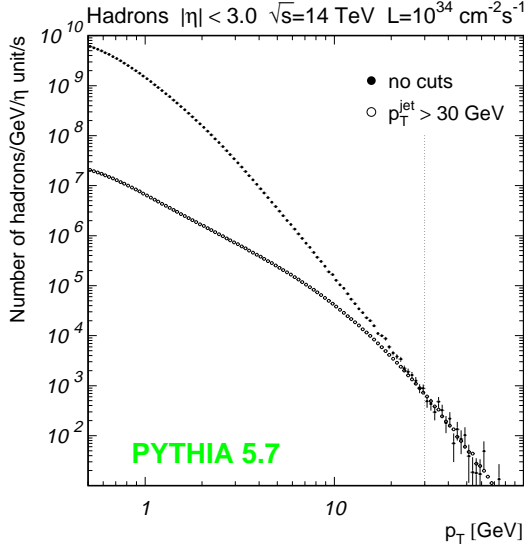


Figure 20: Minimum bias hadrons generated with PYTHIA in p-p collisions at 14 TeV.

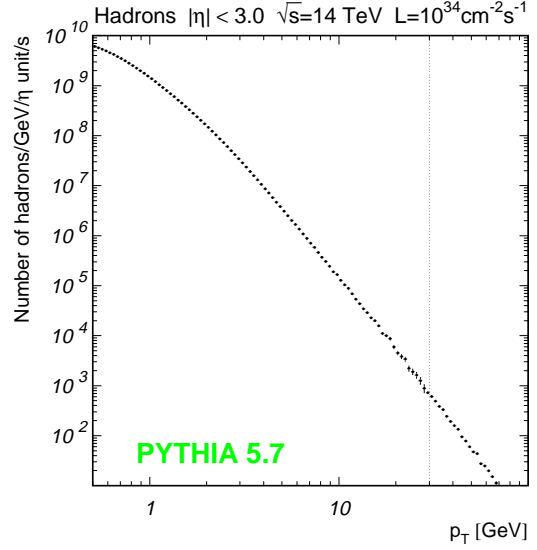


Figure 21: The p_t spectrum of hadrons used for parametrization.

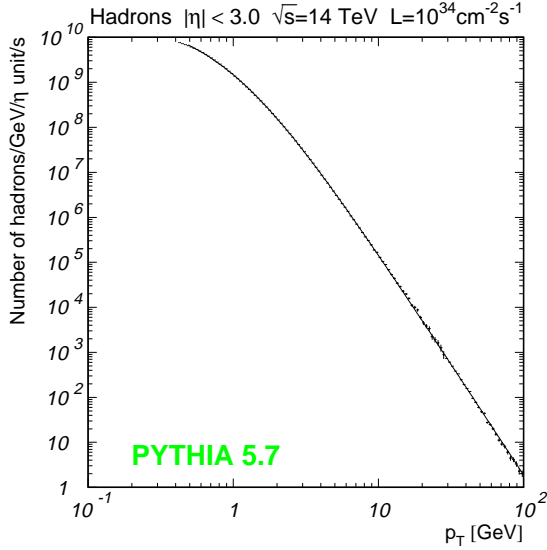


Figure 22: Parametrized rate of minimum bias hadrons.

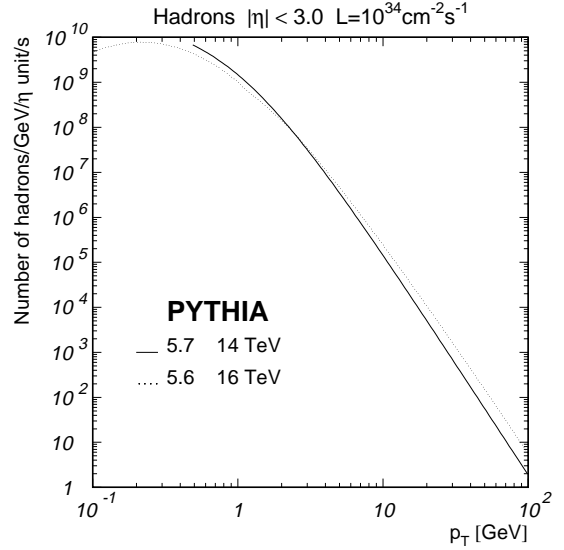


Figure 23: Comparison of new hadron rates with previous parametrization.

Similar procedure has been used to parametrize the prompt muon spectrum. It is seen in Fig. 24 that for the minimum bias muons only (full circles) statistics above 10 GeV is not sufficient to enable accurate parametrization. Thus it was necessary to generate additional hard events of $p_t^{jet} > 10$ GeV and $p_t^{jet} > 30$ GeV (see Table 1). Finally, the distribution to be parametrized, consisted of muons with:

- $p_t < 5$ GeV from minimum bias sample without p_t^{jet} cuts,
- $5 \text{ GeV} < p_t < 20$ GeV from $p_t^{jet} > 10$ GeV sample,
- $p_t > 20$ GeV from $p_t^{jet} > 30$ GeV sample and is plotted in Fig. 25.

In this case the p_t spectrum of muons is a lognormal distribution:

$$\frac{dN}{d\eta dp_t} = a \exp \left[- \frac{(x - \mu)^2}{2\sigma^2} \right]$$

where

$$x = \log_{10} p_t [\text{GeV}], \quad a = 1.3084 \cdot 10^6, \quad \mu = -0.7250, \quad \sigma = 0.4333.$$

It is illustrated in Fig. 26.

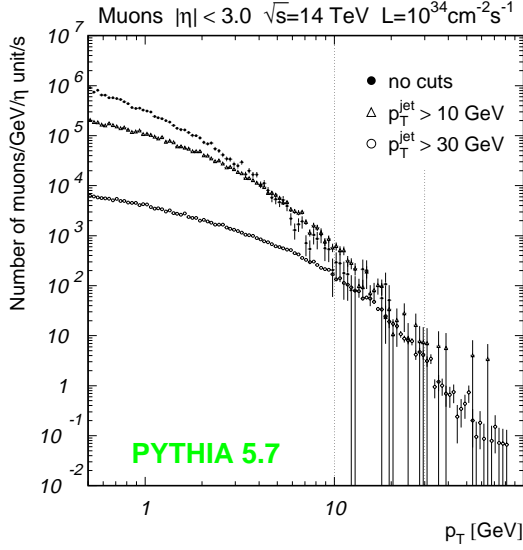


Figure 24: Minimum bias muons generated with PYTHIA in p-p collisions at 14 TeV.

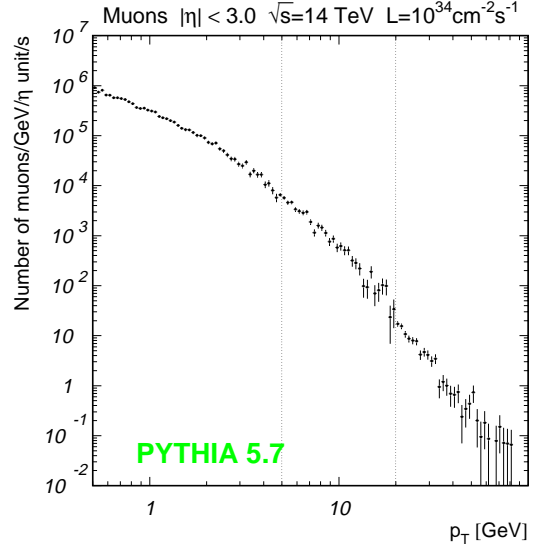


Figure 25: The p_t spectrum of muons used for parametrization.

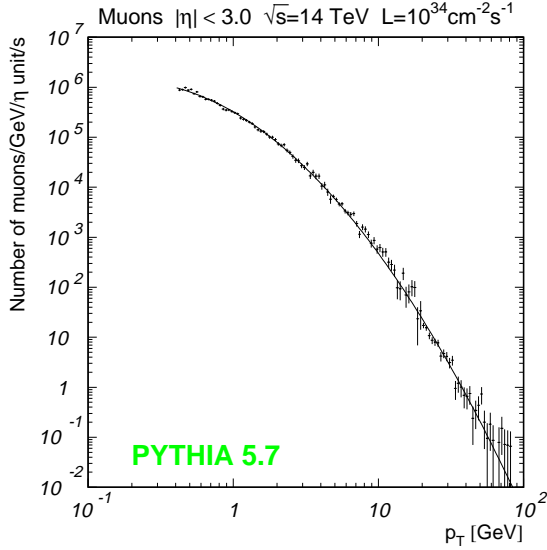


Figure 26: Parametrized rate of minimum bias muons.

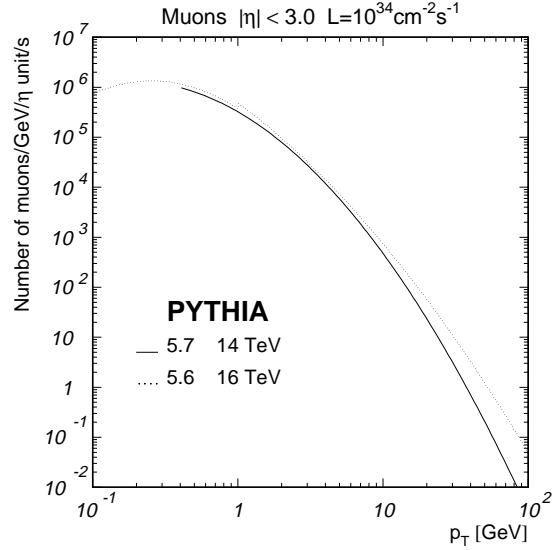


Figure 27: Comparison of new muon rates with previous parametrization.

The data have been fitted from $p_t = 0.4$ GeV to $p_t = 100$ GeV, but both formulae have a good asymptotic behaviour and can be used up to $p_t \rightarrow +\infty$. The parametrisations are not valid for $p_t < 0.4$ GeV.

In Figures 23 and 27 the new (solid) curves are drawn in comparison with the older (dotted) ones [3]. It is seen that the new cross sections are smaller and the spectra are softer. In order to understand the origin of differences, we repeated the simulation with PYTHIA 5.6 (same parameters as in [2] and [3]) at $\sqrt{s} = 16$ and 14 TeV (see Tab. 3).

Table 3: LHC minimum bias samples simulated with various versions of PYTHIA

PYTHIA	structure f.	\sqrt{s}	other parameters
5.6	EHLQ	16 TeV	"UA1" [4]
5.6	EHLQ	14 TeV	"UA1" [4]
5.7	CTEQ2L	14 TeV	defaults

Two ratios of the obtained rates are plotted in Fig. 28

- open circles — v. 5.6 at 14 TeV / v. 5.6 at 16 TeV
- full circles — v. 5.7 at 14 TeV / v. 5.6 at 16 TeV

It is seen that the change of \sqrt{s} from 16 TeV to 14 TeV has rather small impact on the rates (open circles). In contrast, change of the PYTHIA version (together with its default parameters and structure functions) cause a significant change of the particle spectra (full circles). It should be noticed that the default values of some PYTHIA parameters have been changed in order to reproduce other recent experimental data [5, 12]. The main difference comes probably from replacing the EHLQ structure functions by the CTEQ2L ones [5] which account for the recent HERA results at low x .

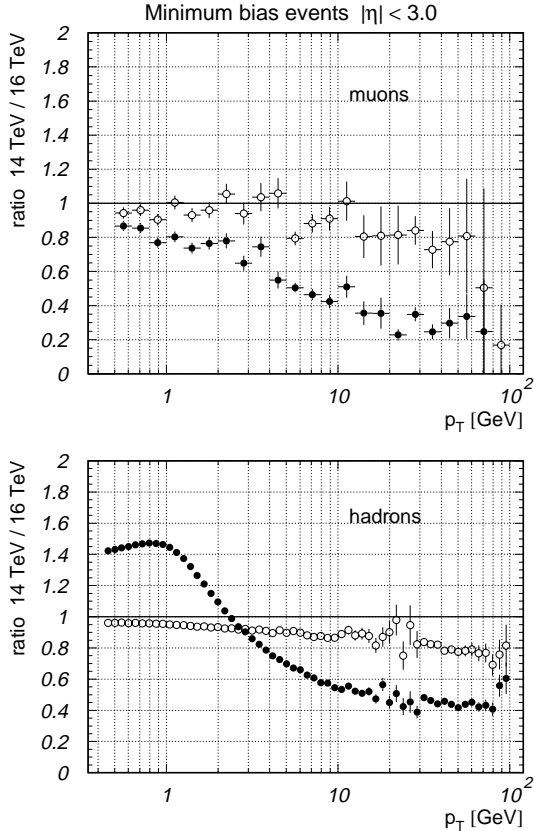


Figure 28: Ratios of rates predicted by PYTHIA: open circles — v. 5.6 at 14 TeV / v. 5.6 at 16 TeV full circles — v. 5.7 at 14 TeV / v. 5.6 at 16 TeV for muons (upper) and hadrons (bottom plot).

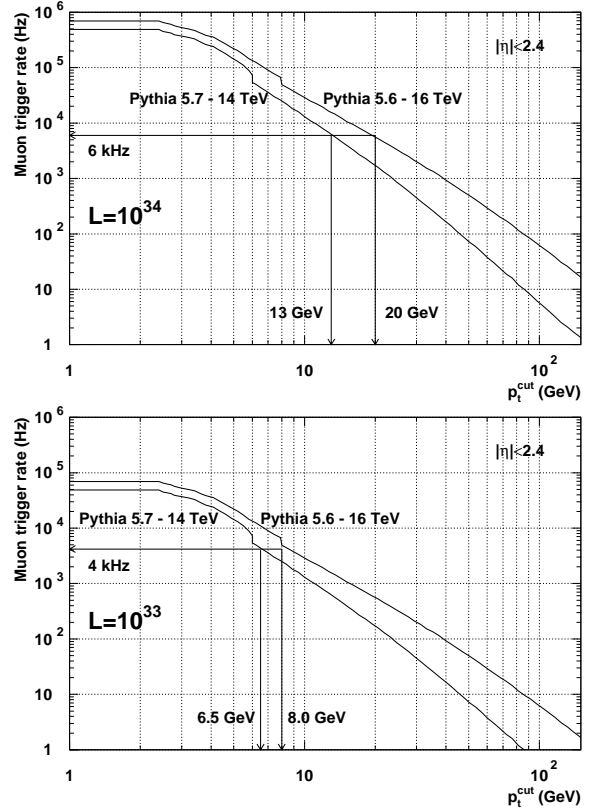


Figure 29: Total single muon trigger rates at $L = 10^{34} \text{ cm}^{-2} \text{ s}^{-1}$ and $L = 10^{33} \text{ cm}^{-2} \text{ s}^{-1}$ for old and new parametrizations.

7 Muon trigger rates in CMS

The particle rates, parametrized as above, have been folded with trigger efficiency [13] in order to get the muon trigger rate. Trigger efficiency has been given by the function **EFFMUTR** available from the **CMSIM** package, version **008**, deck **muon.cmz//muon/muouti/effmutr**. The low p_t algorithm, based on two muon stations in the barrel has been used for $p_t < 6 \text{ GeV}$ [14] instead of $p_t < 8 \text{ GeV}$ assumed in the Technical Proposal [1]. Resulting trigger rates are plotted in Fig. 29. It is seen that the new rates are quite significantly lower than those in the Technical Proposal [1]. If we keep the limits on the single muon trigger rates of 6 kHz and 4 kHz for luminosity $10^{34} \text{ cm}^{-2} \text{ s}^{-1}$ and $10^{33} \text{ cm}^{-2} \text{ s}^{-1}$ respectively, we can lower the corresponding thresholds down to 13 GeV and 6.5 GeV. This may remarkably increase statistics in some physics channels, e.g. $B_d^0 \rightarrow \pi^+ \pi^-$ with a tagging muon trigger. This result, however, should be considered as very preliminary, because the efficiency curves need to be updated according to recent changes in the design.

Conclusions

Inclusive spectra of b-quarks and muons measured in UA1, CDF and D0 experiments have been compared with predictions of PYTHIA 5.7. PYTHIA reproduces the data within a factor 2 or better. This gives us some confidence in extrapolation to the LHC energy. Predicted LHC spectra are softer than those presented in the Technical Proposal [1] which have been obtained with PYTHIA 5.6. Preliminary estimations show that this may allow us to lower the muon trigger thresholds.

Acknowledgment

Authors would like to thank warmly D. Denegri and J. Królikowski for many useful comments and valuable discussions. We are also very grateful to the P. Sphicas for providing us the recent CDF data.

References

- [1] *The Compact Muon Solenoid - Technical Proposal*, CERN/LHCC 94-38, December 1994.
- [2] M. Konecki, J. Królikowski, and G. Wrochna, *Simulation study of the single muon, RPC based trigger for CMS*, CMS TN/92-39.
- [3] D. Chrisman and T. Moers, *A Study of Charged Particle Rates and Muon Backgrounds in the CMS Muon Chambers*, CMS TN/93-106.
- [4] G. Ciapetti and A. Di Caccio, *Monte Carlo Simulation of Minimum Bias Events at the LHC Energy*, Proc. LHC Workshop Aachen, 1990, CERN 90-10.
- [5] T. Sjöstrand, *PYTHIA 5.7 and JETSET 7.4 - Physics and Manual*, CERN-TH.7112/93.
- [6] A. Nisati, *Muon Rates at the LHC*, Proc. LHC Workshop Aachen, 1990, CERN 90-10.
- [7] C. Albajar et al., UA1 Collab., *Z.Phys. C - Particles and Fields* 37, 489-503 (1988); C. Albajar et al., UA1 Collab., *Phys. Lett. B* 256 (1991) 121.
- [8] P. Sphicas, *B Physics at CDF and D0*, talk at the Four Seas Conference, Trieste, June 25-July 1, 1995.
- [9] S. Abachi et al., D0 Collab., *Inclusive Muon and b Quark Production Cross Sections in p \bar{p} Collisions at $\sqrt{s} = 1.8$ TeV*, submitted paper no. 0364 to the EPS HEP Conf., Brussels, July 27-August 2, 1995.
- [10] A.K.A. Maciel, *Photo- and Hadro-production of charm and beauty at Fermilab*, talk at the EPS HEP Conf., Brussels, July 27-August 2, 1995.
- [11] S. Abachi et al., D0 Collab., *Inclusive μ and b-Quark Production Cross Sections in p \bar{p} Collisions at $\sqrt{s} = 1.8$ TeV*, FERMILAB-PUB-409/E, submitted to *Phys. Rev. Lett.*
- [12] G. A. Schuler and T. Sjöstrand, *Phys. Rev. D* 49, 2257, 1994.
- [13] H. Czyrkowski et al., *RPC based CMS muon trigger - progress report*, CMS TN/93-111.
- [14] M. Konecki et al., *RPC geometry and Muon Trigger acceptance*, CMS TN/95-120.